Oxygen Effect in Heterobimetallic Catalysis: The Zr−O−Ti System as an Excellent Example for Olefin Polymerization‡

Prabhuodeyara M. Gurubasavaraj,† Herbert W. Roesky,*,†
Prabhuodeyara M. Veeresha Sharma,# Rainer B. Oswald,§ Volker Dolle,⊥
Regine Herbst-Irmer,† and Aritra Pal†

Institute of Inorganic Chemistry, University of Göttingen, Tammannstrasse 4, 37077 Göttingen, Germany, Institute of Physical Chemistry, University of Göttingen, Tammannstrasse 6, 37077 Göttingen, Germany, Department of Chemistry, Gulbarga University, Gulbarga, India, and Basell R & D Polymer Physics and Characterization, Industriepark, Hoechst, Frankfurt, Germany

Received March 12, 2007

This paper describes the synthesis of a covalently linked oxygen-bridged heterobimetallic complex of zirconium and titanium (**2**) by using the precursors $Cp^*_2ZrMe(OH)$ (**1**) and Cp^*TiMe_3. The crystal structural data show that complexes **1** and **2** crystallize in the orthorhombic and monoclinic system, respectively. Compound **2**, when activated with methylaluminoxane (MAO), shows high activity in ethylene homopolymerization and produces LLDPE. A theoretical study on complex **2** reveals that the bridging oxygen enhances the Lewis acidity at the metal centers. Preliminary investigation of the catalytically active species shows that the initial attack of MAO occurs at the titanium center. Complex **2** exhibits good thermal stability in high-temperature polymerization reactions. The polymer products were characterized by ^{13}C NMR, DSC measurement, and GPC analysis.

Introduction

In recent years there has been immense research interest in preparing catalysts to produce linear low-density polyethylene (LLDPE). This is due to the following significant rheological and mechanical properties of LLDPE compared to the conventional polymers of ethylene: high tensile strength, higher impact and puncture resistance, superior toughness, good organoleptics and low blocking, excellent clarity and gloss, and easy blends with other polyolefins.[1] LLDPE can be obtained from the polymerization of ethylene by using Ziegler−Natta catalysts or by metallocene catalysts, which are formed by the reaction of group 4 metallocenes with a coactivator, of which methylaluminoxane (MAO) is most typical.[2] In the case of conventional Ziegler−Natta catalysts, LLDPE suffers in terms of clarity or stiffness, but by using metallocene catalysis, some long chain branching is introduced, which improves clarity and stiffness.

Typically, LLDPE can be obtained by the copolymerization of ethylene with a linear α-olefin comonomer. LLDPE can also be produced by single-site constrained-geometry catalysts (CGCs),[3] which are based on cooperative effects between active centers in multinuclear complexes. For example Marks et al.[4] reported that the binuclear compounds exhibit higher catalytic activity than the mononuclear complexes. Another approach for olefin polymerization is using "tandem catalysis".[5] In this type of catalysis, two separate single-site olefin polymerization catalysts of zirconium and later transition metals were used in the same system to catalyze the polymerization reaction. The first single-site catalytic center produces oligomers, which are subsequently incorporated into high molecular weight polymers by the second metallic center. Since this type of polymerization requires intermolecular processes, it was speculated that the spatial proximity between two metallic centers might perform such functions more efficiently. For single-site olefin polymerization catalysts two connectivity strategies (electrostatic and

‡ Dedicated to Professor Neil Bartlett on the occasion of his 75th birthday.

* Author to whom correspondence should be addressed. E-mail: hroesky@gwdg.de.
† Institute of Inorganic Chemistry, University of Göttingen.
§ Institute of Physical Chemistry, University of Göttingen.
# Gulbarga University.
⊥ Basell R & D Polymer Physics and Characterization.

(1) See for example: (a) Niaounakis, M.; Kontou, E. *J. Poly. Sci. Polym. Phys.* **2005**, *43*, 1712. (b) James, D. E. In *Encyclopedia of Polymer Science and Engineering*; Mark, H. F., Bikales, N. M., Overberger, C. G., Menges, G., Eds.; Wiley-Interscience: New York, 1985; Vol. 6, pp 429−454. (c) Kulshrestha, A. K.; Talapatra, S. In *Handbook of Polyolefins*; Vasile, C., Ed.; Marcel Dekker: New York, 2000; pp 1−70. (d) Cran, M. J.; Bigger, S. W. *J. Plast. Film Sheeting* **2006**, *22*, 121. (e) Jin, H.-J.; Kim, S.; Yoon, J.-S. *J. Appl. Polym. Sci.* **2002**, *84*, 1566. (f) Starck, P.; Malmberg, A.; Lofgren, B. *J. Appl. Polym. Sci.* **2002**, *83*, 1140. (g) Quijada, R.; Narvaez, A.; Rojas, R.; Rabagliati, F. M.; Galland, G. B.; Maules, R. S.; Benabente, R.; Perez, E.; Perena, J.; Bello, A. *Macromol. Chem. Phys.* **1999**, *200*, 1306. (h) Galland, G. B.; Seferin, M.; Mauler, R. S.; Dos, S.; Joao H. Z. *Polym. Int.* **1999**, *48*, 660. (i) Quijada, R.; Scipioni, R.; Mauler, R.; Galland, G.; Miranda, M. S. *Polym. Bull.* **1995**, *35*, 299. (j) Quijada, R.; Dupont, J.; Lacerda, M.; Scipione, R.; Galland, G. *Macromol. Chem. Phys.* **1995**, *196*, 3991.

(2) (a) Brintzinger, H. H.; Fischer, D.; Mülhaupt, R.; Rieger, B.; Waymouth, R. M. *Angew. Chem., Int. Ed. Engl.* **1995**, *34*, 1143. (b) *Ziegler Catalysts*; Fink, G., Mülhaupt, R., Brintzinger, H. H., Eds.; Springer-Verlag: Berlin, 1995.

(3) See for example: (a) Iedema, P. D.; Hoefsloot, H. C. J. *Macromolecules* **2003**, *36*, 6632. (b) Klosin, J.; Kruper, W. J., Jr.; Nickias, P. N.; Roof, G. R.; De Waele, P.; Abboud, K. A. *Organometallics* **2001**, *20*, 2663. (c) McKnight, A. L.; Waymouth, R. M. *Chem. Rev.* **1998**, *98*, 2587.

(4) (a) Wang, J.; Li, H.; Guo, N.; Li, L.; Stern, C. L.; Marks, T. J. *Organometallics* **2004**, *23*, 5112. (b) Abramo, G. P.; Li, L.; Marks, T. J. *J. Am. Chem. Soc.* **2002**, *124*, 13966.

(5) (a) Komon, Z. J. A.; Diamond, G. M.; Leclerc, M. K.; Murphy, V.; Okazaki, M.; Bazan, G. C. *J. Am. Chem. Soc.* **2002**, *124*, 15280. (b) Quijada, R.; Rojas, R.; Bazan, G. C.; Komon, Z. J. A.; Mauler, R. S.; Galland. G. B. *Macromolecules* **2001**, *34*, 2411. (c) Komon, Z. J. A.; Bu, X.-H.; Bazan, G. C. *J. Am. Chem. Soc.* **2000**, *122*, 1830. (d) Komon, Z. J. A.; Bu, X.-H.; Bazan, G. C. *J. Am. Chem. Soc.* **2000**, *122*, 12379. (e) Chen, E.-Y.; Marks, T. J. *Chem. Rev.* **2000**, *100*, 1391. (f) Alt, H. G.; Köppl, A. *Chem. Rev.* **2000**, *100*, 1205. (g) Britovsek, G. J. P.; Gibson, V. C.; Wass, D. F. *Angew. Chem., Int. Ed.* **1999**, *38*, 428. (h) Chen, E.-Y.; Metz, M. V.; Li, L.; Stern, C. L.; Marks, T. J. *J. Am. Chem. Soc.* **1998**, *120*, 6287. (i) Komon, Z. J. A.; Bazan, G. C. *Macromol. Rapid Commun.* **2001**, *22*, 467. (j) de Souza, R. F.; Casagrande, O. L., Jr. *Macromol. Rapid Commun.* **2001**, *22*, 1293. (k) Barnhart, R. W.; Bazan, G. C. *J. Am. Chem. Soc.* **1998**, *120*, 1082.

10.1021/om070235k CCC: $37.00
Publication on Web 06/07/2007

covalent) have been pursued to achieve cooperative effects via multinuclear complexes.[3] It was assumed that the dicationic bimetallic framework exhibits enhanced comonomer binding affinity. Therefore the attractive possibility of bringing two catalytic centers in close constrained proximity offers the potential for significantly enhanced catalytic efficiency. Stereoregularity and molecular weight of the polymers can be controlled by changing the environment on the ligand surrounding the metal centers (e.g., by introducing the bulky substitutents on the Cp ring or by an intraanular bridge), which in turn leads to the different specificities of the active species.[5] There are some examples of olefin polymerization known, using heterobimetallic complexes where bis(cyclopentadienyl) M (M = Zr, Hf) moieties are connected to other transition metals via cyclopentadienyl, phosphido, nitrogen ligands, and some alkoxide groups.[6] However, significant enhancement in catalytic activity has rarely been observed even at high temperatures and pressure. Recently we have reported a class of oxygen-bridged heterobimetallic complexes containing an Al−O−M moiety (M = Zr, Ti, Hf), which are highly active in olefin polymerization.[7] To the best of our knowledge, there are no reports of heterobimetallic oxygen-bridged complexes of zirconium and titanium for olefin polymerization.

In this contribution, we report a facile route for the preparation and catalytic property of a Ti−O−Zr-containing compound by the reaction of a tailor-made precursor such as $Cp^*_2ZrMe(OH)$ ($Cp^* = C_5Me_5$) and the titanium component. The heterobimetallic complex (**2**) exhibits high activity toward ethylene polymerization and produces linear low-density polyethylene (LLDPE).

Results and Discussion

Synthesis of $Cp^*_2ZrMe(OH)$ (1). The controlled hydrolysis of $Cp^*_2ZrMe_2$ with 1 equiv of water resulted in the formation of $Cp^*_2ZrMe(OH)$ (**1**) in high yield with the elimination of methane (Scheme 1).

Scheme 1

$$Cp^*_2ZrMe_2 + H_2O \xrightarrow[-\ CH_4]{-30\,^\circ C \text{ to RT},\ n\text{-hexane}} Cp^*_2ZrMe(OH)$$

$Cp^* = C_5Me_5$ **1**

Compound **1** is the first zirconium compound that is bonded to a methyl and OH group at the same zirconium atom. Interestingly, **1** is monomeric in the solid state, and even more strikingly Me and OH groups are not involved in any kind of hydrogen bonding, as shown by X-ray structural analysis and IR spectroscopy. To our surprise compound **1** is unexpectedly stable and does not eliminate methane even at elevated temperatures to form an oxo-bridged complex, unlike $Cp^*_2ZrH_2$, which gives an oxo-bridged complex under elimination of H_2 when treated with water in a 2:1 stoichiometry.[8] The reaction of **1** with 1 equiv of Cp^*ZrMe_2 did not occur. This may be due to the fact that the zirconium center is surrounded by sterically bulky Cp* ligands, which prevent complex **1** from dimerizing with loss of water.

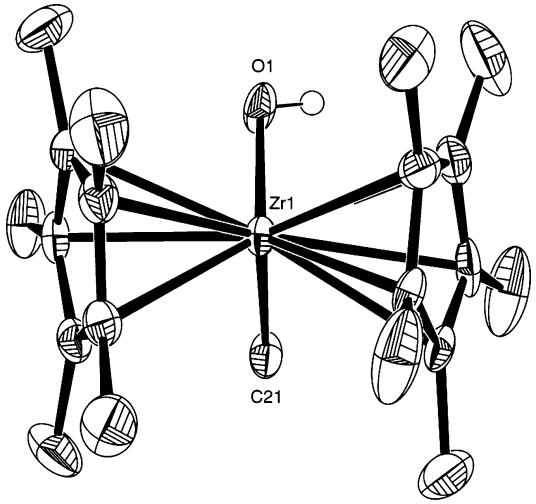

Figure 1. Molecular structure of **1**. Thermal ellipsoids are set at the 50% probability level. H atoms, except for the OH group, are omitted for clarity.

Compound **1** is sensitive to air and hydrolyzes to dihydroxide on exposure to moisture. Complex **2** is soluble in hexane, toluene, ether, tetrahydrofuran, and dichloromethane. It was characterized by EI mass spectrometry, elemental analysis, ^1H and ^{13}C NMR, and IR spectroscopy. The ^1H NMR spectrum of **1** reveals a singlet for CH_3 protons (−0.2 ppm), which appears at remarkably low field as compared with the CH_3 protons (−0.62 ppm) of $Cp^*_2ZrMe_2$. This can be explained by considering the electron affinity of the oxygen in the OH group attached to the Zr center. A single resonance (1.8 ppm) is observed for the methyl protons of the Cp* rings. The presence of the hydroxyl group is confirmed by a resonance of the OH proton (4.2 ppm) and an O−H stretching mode (3680 cm^{-1}) in the IR spectrum. The MS spectrum of compound **1** is interesting when compared to that of $Cp^*_2Zr(OH)_2$,[9] which gives an intense peak at *m*/*z* 376 (^{90}Zr) corresponding to the oxozirconium cation $[Cp^*_2ZrO]^+$, whereas compound **1** shows an intense peak at *m*/*z* 377 (^{90}Zr) corresponding to $[M^+ - Me]$. This indicates the low acidic character of the proton attached to oxygen, obviously due to the strong electron-donating nature of the methyl group.

Molecular Structure of 1. Crystals of **1** suitable for X-ray structural analysis were obtained from *n*-hexane at −20 °C. Compound **1** crystallizes in the orthorhombic space group $P2_12_12_1$. The Zr center is bonded to two Cp* groups and to two ancillary ligands (Me and OH) adopting a distorted tetrahedral geometry around the metal (Figure 1). The OH and methyl positions and also one Cp* ring are disordered. The O(1)−Zr(1)−C(21) bond angle (95.5(2)°) and the angle involving the centroids of the Cp*rings (137.6°) are comparable to those of $Cp^*_2Zr(OH)_2$[9] (O−Zr−O, av 98.9(2)° and Cp* angle av 137.7(5)°), suggesting a steric interaction between the methyl−methyl groups of the Cp* ligands.

Theoretical Study on Compound 1. To further investigate the bonding situation around the zirconium atom and to know the reason for the unusual stability of compound **1** compared to $Cp^*_2ZrH(OH)$, which could not be isolated, an NBO analysis including donor and acceptor interactions has been performed for the molecules. This analysis shows that the compounds vary significantly in the charge on the central atom. For compound **1** the charge is 1.82, and for $Cp^*_2ZrH(OH)$, it is 1.58. Compound **1** has a Zr−C bond that can best be described as polar covalent.

(6) Ishino, H.; Takemoto, S.; Hirata, K.; Kanaizuka, U.; Hidai, M.; Nabika, M.; Seki, Y.; Miyatake, T.; Suzuki, N. *Organometallics* **2004**, *23*, 4544.

(7) (a) Bai, G.; Singh, S.; Roesky, H. W.; Noltemeyer, M.; Schmidt, H.-G. *J. Am. Chem. Soc.* **2005**, *127*, 3449. (b) Gurubasavaraj, P. M.; Mandal, S. K.; Roesky, H. W.; Oswald, R. B.; Pal, A.; Noltemeyer, M. *Inorg. Chem.* **2007**, *46*, 1056.

(8) Hillhouse, G. L.; Bercaw, J. E. *J. Am. Chem. Soc.* **1984**, *106*, 5472.

(9) Bortolin, R.; Patel, V.; Munday, I.; Taylor, N. J.; Carty, A. J. *J. Chem. Soc., Chem. Commun.* **1985**, 456.

Scheme 2

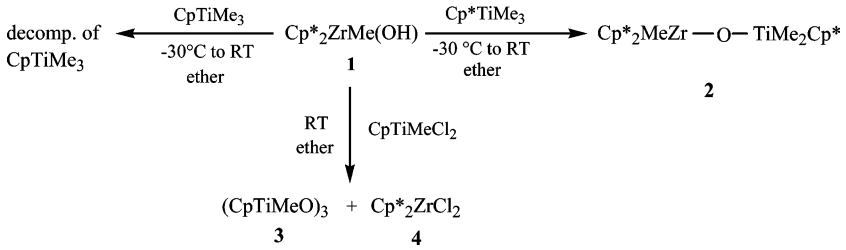

The small charge value of 1.58 for compound $Cp^*_2ZrH(OH)$ is a result of the hydrogen atom, which carries a small negative charge of −0.30, thus leading to a hydridic character.

The weak acid strength of these compounds can be put into an order by taking into account the two-electron stabilization interactions of the O−H bond with other molecular orbitals, which can be described as a donor−acceptor interaction. Summing up all the contributions, the ordering is **1** (33.3 kcal/mol) > $Cp^*_2ZrH(OH)$ (29.6 kcal/mol), with **1** being the weakest acid. As a consequence, the stability of complex **1** can be attributed to the weak acidic character of the proton in OH and the steric bulkiness of the Cp* ligands.

Reactivity of Compound 1: Synthesis of $Cp^*_2MeZr-O-TiMe_2Cp^*$ (2). The unusual kinetic stability of **1** allows its further reactions with a variety of titanium complexes. It reacts under elimination of only one molecule of methane. Complex **1** does not react with $CpTiMe_3$ in ether at −30 °C, and at room temperature, $CpTiMe_3$ decomposes due to its thermal instability to a black precipitate. Similar reaction of complex **1** with $CpTiMeCl_2$ at room temperature yielded $(CpTiMeO)_3$ (**3**) and $Cp^*_2ZrCl_2$ (**4**) (Scheme 2). The crystal data of **4** are in good agreement with the literature.[15]

Complex **1** reacts cleanly with Cp^*TiMe_3 at room temperature under elimination of methane to form the heterobimetallic compound **2** with a Zr−O−Ti moiety (Scheme 2) in good yield. The reaction of **1** with 2 equiv of Cp^*TiMe_3 resulted in the formation of the bimetallic compound **2**. This may be due to the steric crowding of Cp*, which hinders the further reaction to yield a trimetallic compound. When a solution of Cp^*TiMe_3 in ether was added drop by drop to the solution of **1** in ether (−30 °C), a precipitate was formed. After stirring at room temperature for 12 h the solvent was removed in vacuum and the crude product was washed with *n*-hexane.

Compound **2** forms Cp*ZrMe(OH) (**1**) and an unidentified side product, when exposed to moisture. Complex **2** is insoluble in *n*-hexane and pentane but sparingly soluble in toluene, diethyl ether, and THF at room temperature, whereas it dissolves in hot toluene. Complex **2** was thoroughly characterized by ^1H and ^{13}C NMR spectroscopy, EI mass spectrometry, and elemental analysis. The ^1H NMR spectrum of **2** shows two singlets (0.22 and 0.4 ppm) that can be assigned to the Me protons of $TiMe_2$ and ZrMe, respectively, whereas the methyl protons on Cp* of Zr and Ti resonate as two different singlets (1.8 and 2.2 ppm, respectively). The EI mass spectrum (^{90}Zr) exhibits an intense peak at *m*/*z* 574 $[M - 2Me]^+$, and the peak at *m*/*z* 589 (6%) was assigned to $[M - Me]^+$.

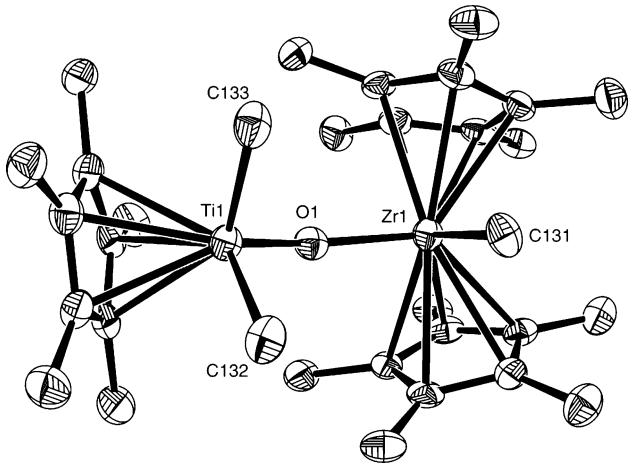

Figure 2. Molecular structure of **2**. Thermal ellipsoids are set at the 50% probability level. H atoms, except for the OH group, are omitted for clarity.

Molecular Structure Description of 2. Suitable crystals for X-ray structural analysis were obtained by cooling the hot toluene solution of **2**. Complex **2** crystallizes as a nonmerohedral twin in the monoclinic space group *Pc* with two nearly identical molecules in the asymmetric unit. The molecular structure is shown in Figure 2.

Compound **2** exhibits a bent Zr−O−Ti core. The Zr and Ti show highly distorted tetrahedral geometry. The coordination sphere of the Zr center consists of two Cp* ligands, one Me group, and one (μ-O) unit, while that of the Ti has a Cp* ligand, two Me groups, and one (μ-O) unit. The Me groups on Ti and Zr are in a staggered conformation. The Zr−C(131) bond distance (2.295(6) Å) is comparable to the average Zr−C bond length in the complex $Cp_2Zr(CH_2SiMe_3)_2$[10] (av 2.284 Å) but is longer than the (av 2.251 Å) value found for $(\eta^5\text{-}C_9H_7)_2ZrMe_2$.[10] The Zr(1)−O(1)−Ti(1) bond angle (av 155.9°) is significantly narrower when compared with the homobimetallic M−O−M angle (M = Zr, Ti) in compounds $(Cp_2ZrMe)_2(\mu\text{-O})$ (174.1(3)°)[10] and $[Cp_2Ti(CF_3C{=}C(H)CF_3)]_2(\mu\text{-O})$ (170.0(2)°).[11] The angle between the centroids of Cp* and the Zr center (134.1°) is also smaller when compared with that of compound **1** (137.6°) and the zirconium dihydroxide (137.7(5)°).[9] However, these angles are much wider than those of highly sterically congested alkoxide-bridged clusters $(Ti_4Zr_2O_4(OBu)_n(OMc)_{10}$ (OMc = methacrylate, n = 2, 4, 6) (98.8(2)° to 108.61(8)°)).[12] The Zr(1)−O(1) (2.022(4) Å) bond distance is slightly longer when compared with the corresponding oxygen-bridged (μ-O) compound $(Cp_2ZrL_2)_2(\mu\text{-O})$ (L = Me, SC_6H_5) (1.945(1) and 1.966(5) Å)[10] but shorter than those of heterobimetallic alkoxide-bridged clusters $((Ti_4Zr_2O_4(OBu)_n(OMc)_{10}$ (n = 2, 4, 6), Zr−O, av 2.189(2) Å).[12] The Ti(1)−O(1) (1.816(4) Å) bond distance is slightly shorter than those in the (μ-O) compound $[Cp_2Ti(CF_3C{=}C(H)CF_3)]_2(\mu\text{-O})$ (av Ti−O, 1.856(6) Å)[11] and alkoxide-bridged cluster $((Ti_4Zr_2O_4(OBu)_n(OMc)_{10}$ (n = 2, 4, 6), Ti−O, av 2.041(5) Å).[12]

Reactivity of Compound 2. To study the reactivity of compound **2**, we carried out further reaction of **2** with LAlMeOH

(10) Hunter, W. E.; Hrncir, D. C.; Bynum, R. V.; Penttila, R. A.; Atwood, J. L. *Organometallics* **1983**, *2*, 750.
(11) Rausch, M. D.; Sikora, D. J.; Hrncir, D. C.; Hunter, W. E.; Atwood, J. L. *Inorg. Chem.* **1980**, *19*, 3817.
(12) Moraru, B.; Kickelbick, G.; Schubert, U. *Eur. J. Inorg. Chem.* **2001**, 1295.

Table 1. Crystal Data and Structure Refinement for Compounds 1 and 2

	1	**2**
formula	$C_{21}H_{34}OZr$	$C_{33}H_{54}OTiZr$
fw	393.7	605.88
color	colorless	yellow
cryst syst	orthorhombic	monoclinic
space group	$P2_12_12_1$	Pc
a, Å	8.035(2)	8.601(2)
b, Å	10.948(3)	15.399(2)
c, Å	22.256(3)	23.084(3)
α, deg	90	90.0
β, deg	90	94.41(2)
γ, deg	90	90.0
V, Å^3	1958(1)	3048.3(9)
Z	4	4
ρ_{calc}, Mg m^{-3}	1.336	1.320
μ, mm^{-1}	0.565	5.184
F(000)	832	1288
θ range for data collection, deg	1.83 to 26.39	2.87 to 59.42
index ranges	$-10 \le h \le 10$ $0 \le k \le 13$ $0 \le l \le 27$	$-9 \le h \le 9$ $-16 \le k \le 17$ $-25 \le l \le 25$
no. of reflns collcd	36 648	52 720
no. of indepnt reflns (R_{int})	4003	11 233
refinement method	full-matrix least-squares on F^2	full-matrix least-squares on F^2
R1, wR2 (all data)	0.0250, 0.0625	0.0496, 0.1325
largest diff peak, hole, e Å^{-3}	−0.433/+0.782	−0.799/+0.551

Table 2. Selected Bond Distances (Å) and Angles (deg) for Compounds 1 and 2

	Compound **1**		
Zr(1)−O(1)	2.040(4)	O(1)−Zr(1)−C(21)	95.5(2)
Zr(1)−C(21)	2.302(7)	X_{Cp*1}−Zr−X_{Cp*2}[a]	137.6
	Compound **2**		
Zr(1)−O(1)	2.022(4)	Zr(1)−O(1)−Ti(1)	156.1(2)
Ti(1)−O(1)	1.816(4)	X_{Cp*1}−Zr(1)−X_{Cp*2}	134.1
Zr(1)−X_{Cp*1}	2.289	O(1)−Zr(1)−C(131)	94.8(2)
Zr(1)−X_{Cp*2}	2.269	O(1)−Ti(1)−C(132)	106.3(2)
Ti(1)−X_{Cp*}	2.092	O(1)−Ti(1)−C(133)	105.3(2)
Zr(1)−C(131)	2.295(6)		
Ti(1)−C(132)	2.120(6)		
Ti(1)−C(133)	2.123(6)		

[a] X_{Cp} = centroid of the Cp ring.

[L = CH(N(Ar)(CMe))$_2$, Ar = 2,6-*i*Pr$_2$C$_6$H$_3$] at room temperature. However, the reaction did not occur even at refluxing the reaction mixture for 24 h. Only the decomposition of LAlMeOH to nacnac has been observed (Scheme 3).

Scheme 3

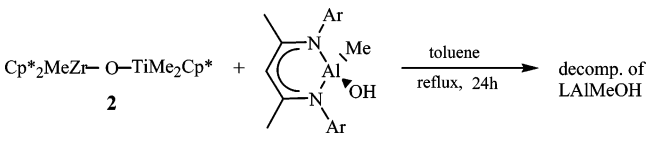

Polymerization of Ethylene by Cp*$_2$MeZr−O−TiMe$_2$Cp* (2). Compound **2** catalyzes the polymerization of ethylene in toluene when activated with MAO. All polymeric materials were isolated as white powders. Table 3 represents the results of ethylene polymerization data. Figure 3 exhibits a graph of activity against the MAO to catalyst ratio of **2**. The polymerization data exhibit that complex **2** is very active even at low (86:1) MAO to catalyst ratio. This high activity of **2** may be due to the bridging oxygen, which enhances the Lewis acidity at the metal centers.

Table 3. Ethylene Polymerization Data for 2[a]

catalyst	MAO: catalyst	t (min)	T (°C)	PE (g)	A ($\times 10^6$)	M_w	M_w/M_n	T_m[b] (°C)
2	86	20	25	1.6	0.25	178 523	4.17	124.0
2	172	20	25	2.4	0.37	105 149	3.42	120.0
2	345	20	25	3.1	0.48			124.5
2	461	20	25	5.5	0.85			124.9
2	518	20	25	6.3	0.97			122.2
2[c]	172	10	83	1.5	0.69			124.1

[a] Polymerization conditions: **2** = 19.8 μmol, 100 mL of toluene at 25 °C, at 1 atm ethylene pressure. Activity (A) = g PE/mol cat·h. [b] DSC. [c] Polymerization conditions: **2** = 13.2 μmol, 83 °C, at 1 atm ethylene pressure.

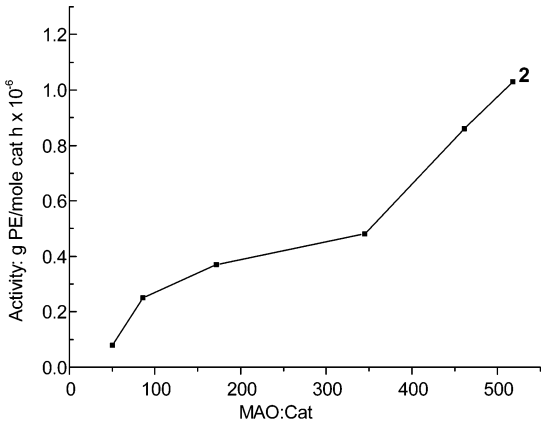

Figure 3. Graph of activity against MAO to catalyst ratios of **2**.

Polymer Properties. DSC measurements show that the melting points (T_m) of the polyethylene produced by **2** are in the range 120 to 125 °C, which is in the typical range for LLDPE. The GPC measurements are monomodal for measured polyethylene samples. The M_w values are low and PDI are broad, which may be due to the fact that a good amount of the products coming from the titanium site are not incorporated into the growing polyethylene chain governed by the zirconium site. Polymerization data of complex **2** indicate high activity but less incorporation of ethylene into the growing polyethylene chain. It can be assumed that two active sites compete for ethylene, leading to the formation of lower molecular weight polyethylene, which makes the PDI broad.

The ^{13}C NMR data exhibit a resonance at 30.12, which corresponds to the backbone carbon of the linear low-density polyethylene. The resonances at 14.44, 23.08, and 32.36 are assigned to C1, C2, and C3, respectively, of the alkyl end group of the polyethylene.

Thermal Stability. For efficient catalytic processes, the ideal situation is that the catalyst has to be both highly active and thermally stable. Good stability of the complex at high temperature is one crucial factor for the application of metallocene complexes on an industrial scale for olefin polymerization.[13] To investigate the thermal stability of complex **2**, polymerization was carried out at high temperature (83 °C). The complex exhibits good thermal stability and shows an increase in activity by almost 2 times that at room temperature (see Table 3). One reasonable explanation is the high oxophilicity of Zr and Ti, which forms strong metal−oxygen bonds and keeps the molecule intact. Furthermore, the sterically bulky and electron-donating Cp* ligands stabilize the cation formed during the catalytic process.

(13) Jia, L.; Yang, X.; Stern, C. L.; Marks, T. J. *Organometallics* **1997**, *16*, 842.

Preliminary Investigation of the Catalytic Species. An attempt was made to monitor the catalytic species formed during the activation of **2** with MAO by ^{1}H NMR spectroscopy at room temperature. Preliminary investigation of the ^{1}H NMR (MAO/**2** = 10) exhibits the downfield shift for the Ti−Me (from 0.22 to 0.45 ppm), and it is accompanied by concomitant broadening of the Ti−Me signal. The initial 2:1 relative intensity of Ti−Me protons when compared with that of Zr−Me protons in **2** is reduced to 1:1 after the addition of MAO. This clearly suggests that one of the methyl groups attached to the Ti center interacts with Al of MAO probably by forming a monocationic bridged complex $[Cp^*_2Zr(Me)OTi(Me)Cp^*(\mu\text{-}Me)AlMe_2]^+$-$[Me-MAO]^-$. The resonance for the bridged methyl is observed at −0.3 ppm. The methyl of the $AlMe_3$−MAO resonates at −0.73 ppm. The resonances for methyl protons of the Cp* rings remain unchanged. These observations are in good agreement with those reported in the literature.[14] The Zr−Me resonance remains unaffected with a slight downfield shift (0.4 to 0.5 ppm), indicating that the Zr−Me does not interact with Al of MAO at such a low concentration of MAO. However, a gradual increase of MAO with **2** (MAO/**2** = 20) results in broad resonances for the Zr−Me and Ti−Me groups, indicating the involvement of Zr to form a dicationic heterobimetallic framework.[4b]

Results of Computational Studies on Complex 2. It is evident from the crystal structure data that the M−O (M = Zr, Ti) bond length is short. Polymerization data show that the compound exhibits high activity in ethylene polymerization. This may be due to the bridging oxygen, which causes short Zr−O and Ti−O bonds, indicative of high electron density within these bonds. As a consequence, the electron density at the active metal sites decreases, exhibiting enhanced Lewis acidic character. To support our findings from the experimental data, ab initio calculations were carried out to determine the electronic density between Zr−O and Ti−O bonds.

Table 4. Selected Calculated and X-ray Bond Distances (Å) and Bond Angles (deg)

bond length	calcd	X-ray	bond angle	calcd	X-ray
Zr(1)−O(1)	2.039	2.022	Zr(1)−O(1)−Ti(1)	157.37	156.90
Ti(1)−O(1)	1.820	1.816	O(1)−Zr(1)−C(131)	94.89	94.80
Zr(1)−C(131)	2.289	2.295	O(1)−Ti(1)−C(132)	104.69	106.30
Ti(1)−C(132)	2.122	2.120	O(1)−Ti(1)−C(133)	104.74	105.3

As shown in Table 4, the resulting structure compares very well with the data obtained by X-ray diffraction, thus giving a solid foundation for the following bond analysis to describe the bonding situation quite well.

The NBO analysis shows that the bonds formed between the metal atoms and the oxygen lead to a significant buildup of electron density on the oxygen atom. The distribution of electrons can be best described as locating 90% in a p-rich orbital of oxygen and leaving only 10% in a d-orbital of the metal. Figures 4 and 5 of the corresponding bonds show that electron density on the Zr atom is more depleted compared with that of the Ti atom.

This bonding scenario of **2** suggests that the Zr center is more Lewis acidic when compared with that of the Ti center. The NMR experiment reveals that the initial activation by MAO occurs at the titanium atom. This can be explained by the steric bulk of the Cp* ligands around the metal centers and the electronic stabilization of the corresponding cations. The steric bulk of Cp* ligands makes the Zr center kinetically less active toward the initial activation by MAO as compared with that of titanium, which has only one Cp* ligand in its coordination sphere. The high electron density on the titanium stabilizes its cation.

(14) Talsi, E. P.; Bryliakov, K. P.; Semikolenova, N. V.; Zakharov, V. A.; Ystenes, M.; Rytter, E. *Mendeleev Commun.* **2003**, *2*, 1.

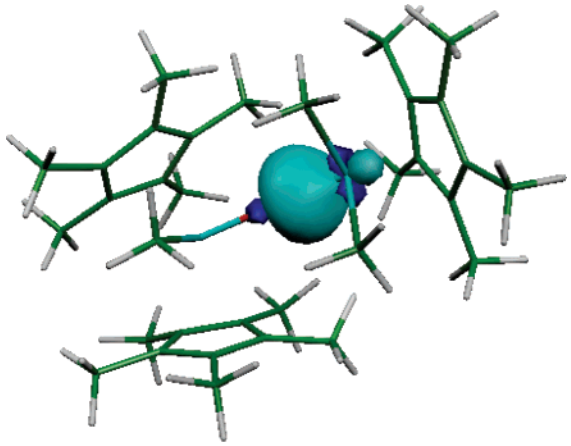

Figure 4. Shape of the bonding orbital between Zr and oxygen.

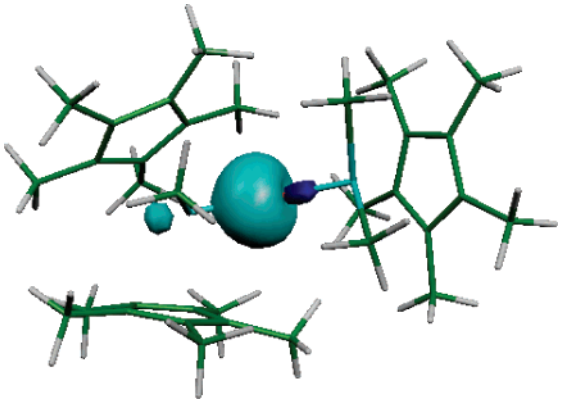

Figure 5. Shape of the bonding orbital between Ti and oxygen.

Conclusions

In this contribution, we report on the synthesis of the kinetically stable $Cp^*_2ZrMe(OH)$ (**1**). This compound was used to prepare the oxygen-bridged heterobimetallic metallocene catalyst containing the Zr−O−Ti unit. The latter was used in ethylene polymerization. The Zr−O−Ti complex (**2**) exhibits thermal stability and high activity in the polymerization and produces LLDPE. A theoretical study reveals that the bridging oxygen plays an important role in complex **2**. First, it helps to form a kinetically and thermally stable Zr−O−Ti unit. Second, it enhances the Lewis acidity at the metallic centers and in turn leads to an increase in its catalytic activity. Further study of this type of catalysts for their use in copolymerization reactions is under investigation in our laboratory.

Experimental Section

General Comments. All experimental manipulations were carried out under an atmosphere of dry argon using standard Schlenk techniques. The samples for spectral measurements were prepared in a glovebox. The solvents were purified according to conventional procedures and were freshly distilled prior to use. $Cp^*_2ZrCl_2$,[15] $Cp^*_2ZrMe_2$,[16] Cp^*TiMe_3,[17a] and $CpTiMeCl_2$[17b] were prepared by procedures that were published elsewhere. Cp^*TiCl_3 was purchased from Aldrich. NMR spectra were recorded on a Bruker Avance 500 instrument, and the chemical shifts are reported with reference to tetramethylsilane (TMS). IR spectra were recorded on a Bio-

Rad Digilab FTS-7 spectrometer. Mass spectra were obtained on a Finnigan MAT 8230 spectrometer by the EI technique. Melting points were obtained in sealed capillaries on a Büchi B 540 instrument. Elemental analyses were performed at the Analytical Laboratory of the Institute of Inorganic Chemistry at Göttingen, Germany.

Synthesis of Cp*$_2$ZrMe(OH) (1). Cp*$_2$ZrMe$_2$ (0.5 g, 1.28 mmol) was dissolved in *n*-hexane (30 mL). The resulting solution was cooled to −30 °C, and 1 equiv of H_2O (23 μL) was added rapidly under vigorous stirring. The temperature of the solution was maintained at −30 °C for 10 min, then was slowly warmed to ambient temperature and stirred for another 30 min until methane evolution had ceased. The solvent was removed in vacuum to obtain a colorless crystalline material. Yield: 0.36 g (72%). Mp: 202 °C (dec). IR (KBr): $\tilde{\nu}$ 3680, 2965, 2908, 1492, 1440, 1380, 1262, 1099, 1022, 941, 865, 801 cm^{-1}; ^{1}H NMR (500 MHz, C_6D_6, 25 °C, TMS): δ −0.2 (s, 3H, Zr−CH_3), 1.8 (s, 30H, C_5(CH_3)$_5$), 4.2 (s, 1H, O*H*). ^{13}C NMR (500 MHz, C_7D_8, 25 °C, TMS): δ 118.7 (s, Cp*$_2$, C_{10}), 11.1 (Cp*$_2$Zr, (CH_3)$_{10}$−Cp$_2$), 27.0 (s, CH_3). MS (EI): *m*/*z* (%) 377 (100) [M − Me]$^+$. Anal. (%) Calcd for $C_{21}H_{34}OZr$ (393.72): C 64.06, H 8.70. Found: C 63.86, H 8.62.

Synthesis of Cp*$_2$MeZr−O−TiMe$_2$Cp* (2). A solution of Cp*TiMe$_3$ (0.228 g, 1.00 mmol) in diethyl ether (30 mL) was added dropwise to a solution of **1** (0.394 g, 1.00 mmol) in diethyl ether (30 mL) at −30 °C. The resulting solution was stirred at −30 °C for 5 min and was slowly warmed to ambient temperature. Vigorous methane elimination was noticed with concomitant formation of a precipitate. After stirring for an additional 12 h the solvent was removed in vacuum and the crude product was washed with *n*-hexane, to give a yellow powder. Yield: 0.5 g (64%). Mp: 224 °C (dec). ^{1}H NMR (500 MHz, C_6D_6, 25 °C, TMS): δ 0.22 (s, 6H, Ti−(CH_3)$_2$), 0.4 (s, 3H, Zr−CH_3), 1.8 (s, 30H, C_5(CH_3)$_5$), 2.2 (s, 15H, C_5(CH_3)$_5$). ^{13}C NMR (500 MHz, C_7D_8, 25 °C, TMS): δ 118.2 (s, Cp*$_2$Zr, C_{10}), 12.2 (Cp*Ti, (CH_3)$_5$−Cp), 11.99 (Cp*$_2$Zr, (CH_3)$_{10}$−Cp$_2$), 121.4 (s, Cp*Ti, C_5), 52.3 (s, Ti−(CH_3)$_2$), 34.8 (s, Zr−CH_3). MS (EI): *m*/*z* (%) 574.2 (100) [M − 2Me]$^+$, 589.2 (6%) [M − Me]$^+$. Anal. (%) Calcd for $C_{33}H_{54}OTiZr$ (605.88): C 65.42, H 8.98. Found: C 64.72, H 8.92.

X-ray Structure Determination of 1 and 2. Data for the structure **2** were collected on a Bruker three-circle diffractometer equipped with a SMART 6000 CCD detector. The data for the structure **1** were collected on a STOE IPDS II diffractometer. Intensity measurements were performed on a rapidly cooled crystal. The structures were solved by direct methods (SHELXS-97)[18] and refined with all data by full-matrix least-squares on F^2.[19] The hydrogen atoms on C−H bonds were placed in idealized positions and refined isotropically with a riding model, whereas the non hydrogen atoms were refined anisotropically. The OH and methyl positions and one of the Cp* rings in complex **1** are disordered. The data for **2** were collected on a non-merohedrally twinned crystal. The twin law is a 180° rotation about the reciprocal axis 012. They were refined with distance restraints and restraints for the anisotropic displacement parameters. Crystal data and selected bond lengths and angles are shown in Tables 1 and 2.

Computational Details. The calculations were performed at the well-established DFT level of theory making use of the B3LYP functional[20,21] as implemented in the Gaussian program package[22] employing the LanL2DZ[23]basis set for Zr and Ti and 6-31G[24−26] for the remaining atoms. In the first step the compound was fully optimized to its equilibrium structure. The analysis of the resulting electronic wave function for this structure was then used to obtain the electronic density at the atoms of interest. The analysis of the bonding situation was performed at the calculated equilibrium geometry by means of an NBO analysis.[27−29]

Ethylene Polymerization Experiments. Ethylene polymerizations were carried out on a high vacuum line (10^{-5} Torr) in an autoclave (Buchi). In a typical experiment, the catalyst (see Table 3) was taken and an appropriate amount of MAO (1.6 M, Aldrich) was added, stirring for 20 min for the activation. After stirring the resulting mixture was placed into the autoclave by using a gastight syringe, which was previously filled with 100 mL of toluene under ethylene atmosphere (1 atm). After stirring for an appropriate time, the reaction was quenched using 15% acidified methanol, and the white polyethylene formed was collected by filtration and dried. The results are shown in Table 3.

Polymer Characterization. ^{13}C NMR assays of polymer microstructure were conducted in 1,1,2,2-tetrachloroethane-d_2 at 110 °C. Resonances were assigned according to the literature for polyethylene and ethylene + α-olefin copolymers.

Differential scanning calorimetric measurements of the polymer melting curves were measured on a TA 2920 instrument (modulated differential scanning calorimeter), which was calibrated against indium metal. Typically ca. 4 mg samples were used (10 °C/min).

Gel permeation chromatography (GPC) was carried out at Basell R & D Polymer Physics and Characterization, Industriepark, Hoechst, Frankfurt, Germany. 1,2,4-Trichlorobenzene was used as solvent. The columns were calibrated with narrow molar mass distribution standards of polystyrene.

Acknowledgment. This work is supported by the Göttinger Akademie der Wissenschaften, Deutsche Forschungsgemeinschaft, and the Fonds der Chemischen Industrie. P.M.G. is grateful to Katrin Gehrke for DSC measurement and S. K. Mandal for helping in the preparation of the manuscript.

Supporting Information Available: Ab initio calculation results and complete ref 22. X-ray data (CIF) of **1** and **2**. This material is available free of charge via the Internet at http://pubs.acs.org.

OM070235K

(15) Manriquez, J. M.; McAlister, D. R.; Rosenberg, E.; Shiller, A. M.; Williamson, K. L.; Chan, S. I.; Bercaw, J. E. *J. Am. Chem. Soc.* **1978**, *100*, 3078.

(16) Manriquez, J. M.; McAlister, D. R.; Sanner, R. D.; Bercaw, J. E. *J. Am. Chem. Soc.* **1978**, *100*, 2716.

(17) (a) Mena, M.; Royo, P.; Serrano, R.; Pellinghelli, M. A.; Tiripicchio, A. *Organometallics* **1989**, *8*, 476. (b) Erskine, G. J.; Hurst, G. J. B.; Weinberg, E. L.; Hunter, B. K.; McCowan, J. D. *J. Organomet. Chem.* **1984**, *267* (3), 265.

(18) Sheldrick, G. M. *Acta Crystallogr.* **1990**, *A46*, 467.

(19) Sheldrick, G. M. *SHELXS-97* and *SHELXL-97*, Program for Crystal Structure Refinement; Göttingen University: Göttingen, Germany, 1997.

(20) Lee, C.; Yang, W.; Parr, R. G. *Phys. Rev. B* **1988**, *37*, 785.

(21) Miehlich, B.; Savin, A.; Stoll, H.; Preuss, H. *Chem. Phys. Lett.* **1989**, *157*, 200.

(22) Frisch, M. J.; et al. *Gaussian 03, Revision C.02*; Gaussian, Inc.: Wallingford, CT, 2004.

(23) Hay, P. J.; Wadt, W. R. *J. Chem. Phys.* **1985**, *82*, 270.

(24) Ditchfield, R.; Hehre, W. J.; Pople, J. A. *J. Chem. Phys.* **1971**, *54*, 724.

(25) Hariharan, P. C.; Pople, J. A. *Theor. Chim. Acta* **1973**, *28*, 213.

(26) Rassolov, V. A.; Ratner, M. A.; Pople, J. A.; Redfern, P. C.; Curtiss, L. A. *J. Comput. Chem.* **2001**, *22*, 976.

(27) Foster, J. P.; Weinhold, F. *J. Am. Chem. Soc.* **1980**, *102*, 7211.

(28) Reed, A. E.; Weinhold, F. *J. Chem. Phys.* **1985**, *83*, 1736.

(29) Reed, A. E.; Curtiss, L. A.; Weinhold, F. *Chem. Rev.* **1988**, *88*, 899.